



Contents lists available at ScienceDirect

Ceramics International

journal homepage: [www.elsevier.com/locate/ceramint](http://www.elsevier.com/locate/ceramint)

# Temperature stable (1-x)NaCa<sub>4</sub>V<sub>5</sub>O<sub>17</sub>-xBaV<sub>2</sub>O<sub>6</sub> microwave dielectric ceramics for ULTCC applications

Cuijin Pei<sup>a,\*\*\*</sup>, Yang Li<sup>a</sup>, Jingjing Tan<sup>a</sup>, Guoguang Yao<sup>a,\*</sup>, Yanmin Jia<sup>a,\*\*</sup>, Weihong Liu<sup>a</sup>, Peng Liu<sup>b</sup>, Huaiwu Zhang<sup>c</sup>

<sup>a</sup> School of Science, Xi'an University of Posts and Telecommunications, Xi'an, 710121, China

<sup>b</sup> College of Physics and Information Technology, Shaanxi Normal University, Xi'an, 710062, China

<sup>c</sup> State Key Laboratory of Electronic Thin Films and Integrated Devices, University of Electronic Science and Technology of China, Chengdu, 610054, China

## ARTICLE INFO

### Keywords:

Ultra-low-temperature cofired ceramic  
Composite  
Dielectric properties

## ABSTRACT

Novel temperature stable (1-x)NaCa<sub>4</sub>V<sub>5</sub>O<sub>17</sub>-xBaV<sub>2</sub>O<sub>6</sub> (0.8 ≤ x ≤ 0.9, (1-x)NCV-xBV) ceramics were successfully synthesized through a high-temperature solid phase reaction route. XRD and SEM-EDS analysis demonstrated that only NaCa<sub>4</sub>V<sub>5</sub>O<sub>17</sub> and BaV<sub>2</sub>O<sub>6</sub> phases were formed without any extra phase. The introduction of BaV<sub>2</sub>O<sub>6</sub> not only effectively improved the  $\tau_f$  of NaCa<sub>4</sub>V<sub>5</sub>O<sub>17</sub> matrix but also considerably lowered its sintering temperature to 550 °C. Typically, an approximate-zero  $\tau_f$  value around -1.0 ppm/°C was achieved for 550 °C sintered 0.12NCV-0.88BV ceramics with low  $\epsilon_r$  of 10.9 and Qxf of 15,500 GHz (at 10.3 GHz). Its good compatibility with Al electrode furthermore made 0.12NCV-0.88BV composites suitable for ULTCC applications.

## 1. Introduction

Nowadays, there is a growing care about the microwave dielectric ceramics, which are used in 5G wireless communications as advanced substrates, dielectric radome, dielectric filter et al. [1–3]. As the 5G era is arrival, it puts forward higher requirement for advanced dielectric materials. The dielectric materials owing low dielectric loss or high quality factor (Qxf for frequency selectivity), small dielectric permittivity ( $\epsilon_r$  < 15 for fast signal transmission) and approximate-zero temperature coefficient of resonant frequency ( $\tau_f$  for thermal stability) get the research hotspots [4,5]. Meanwhile, dielectric ceramics owing low heating temperature are demanded by LTCC, even ULTCC technology, which is conducive to compact electronic devices [6–8]. Hence, it is urgently required to develop dielectric materials with superior performances along with low or even ultra-low sintering temperature.

Recently, vanadium-containing compounds aroused researcher's interest once again since their low sintering temperature and good dielectric performances at microwave region [9–13]. Several vanadium host ceramics systems have been investigated for the application in LTCC domains, such as Ba<sub>3</sub>A (V<sub>2</sub>O<sub>7</sub>)<sub>2</sub>, (CaBi) (MoV)O<sub>4</sub>, CaV<sub>2</sub>O<sub>6</sub> et al. Quite recently, Xie et al. [14] reported the fabrication and spectrum properties characterization for NaCa<sub>4</sub>V<sub>5</sub>O<sub>17</sub> with triclinic structure.

Later, Yin et al. first reported the dielectric performances at microwave region ( $\epsilon_r$  = 9.7, Qxf = 51,000 GHz,  $\tau_f$  = -84 ppm/°C) of 840 °C-sintered NaCa<sub>4</sub>V<sub>5</sub>O<sub>17</sub> ceramics, while they also reported the good chemical compatibility of NaCa<sub>4</sub>V<sub>5</sub>O<sub>17</sub> with Ag [15]. Yet, in our research it was found that the poor chemical compatibility between NaCa<sub>4</sub>V<sub>5</sub>O<sub>17</sub> and Ag, when prepared NaCa<sub>4</sub>V<sub>5</sub>O<sub>17</sub> using V<sub>2</sub>O<sub>5</sub> as raw material, which posed challenges for LTCC applications and should be resolved [16]. However, thus far, the possible ULTCC application of NaCa<sub>4</sub>V<sub>5</sub>O<sub>17</sub> has not been investigated. Therefore, in order to make NaCa<sub>4</sub>V<sub>5</sub>O<sub>17</sub> as a possible ULTCC material, the sintering temperature of NaCa<sub>4</sub>V<sub>5</sub>O<sub>17</sub> ceramics should be below the melting point of Al (700 °C). Considering the merits of BaV<sub>2</sub>O<sub>6</sub> with seldom large positive  $\tau_f$  and ultralow sintering temperature of 550 °C [17], it was chose to modulate the  $\tau_f$  and reduce the firing temperature for NaCa<sub>4</sub>V<sub>5</sub>O<sub>17</sub> matrix. In present study, the (1-x)NaCa<sub>4</sub>V<sub>5</sub>O<sub>17</sub>-xBaV<sub>2</sub>O<sub>6</sub> composite ceramics were fabricated, and their sintering behavior, microwave dielectric characterizations were discussed. To assess its possibility in ULTCC technology, we also studied the chemical compatibility between 0.12 NaCa<sub>4</sub>V<sub>5</sub>O<sub>17</sub> -0.88 BaV<sub>2</sub>O<sub>6</sub> and Al electrode.

\* Corresponding author.

\*\* Corresponding author.

\*\*\* Corresponding author.

E-mail addresses: [yaoguoguang@xupt.edu.cn](mailto:yaoguoguang@xupt.edu.cn) (G. Yao), [ymjia@zjnu.edu.cn](mailto:ymjia@zjnu.edu.cn) (Y. Jia).

<https://doi.org/10.1016/j.ceramint.2020.07.250>

Received 21 June 2020; Received in revised form 19 July 2020; Accepted 25 July 2020

0272-8842/ © 2020 Elsevier Ltd and Techna Group S.r.l. All rights reserved.

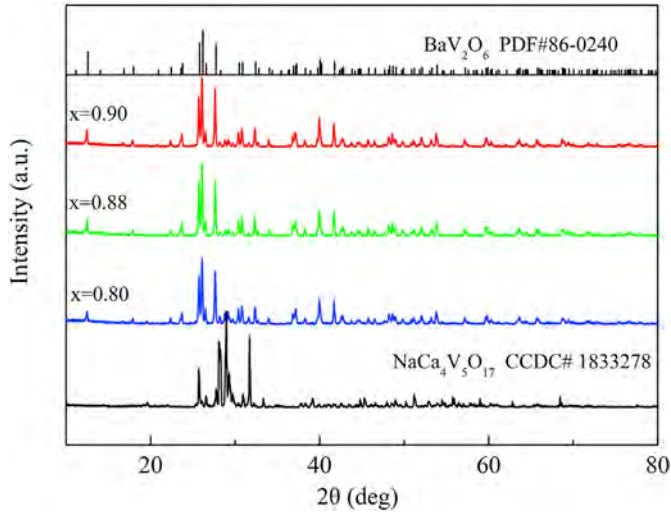


**Fig. 1.** PXRD patterns of 800 °C sintered  $\text{NaCa}_4\text{V}_5\text{O}_{17}$  ceramics and 550 °C sintered  $(1-x)\text{NaCa}_4\text{V}_5\text{O}_{17}-x\text{BaV}_2\text{O}_6$  ( $0.8 \leq x \leq 0.9$ ) ceramics.

**Table 1**

The measured and calculated  $\epsilon_r$  and  $\tau_f$  values of  $(1-x)\text{NaCa}_4\text{V}_5\text{O}_{17}-x\text{BaV}_2\text{O}_6$  ceramics sintered at 550 °C for 4 h.

Composition x	$\epsilon_r$	$\epsilon_{\text{cal}}$	$\tau_f$ (ppm/°C)	$\tau_{f \text{ cal}}$ (ppm/°C)
0.80	10.86	10.74	-12.7	-14.1
0.85	10.96	11.02	1.0	3.0
0.90	10.97	11.10	3.0	8.0

## 2. Experimental procedure

The  $(1-x)\text{NaCa}_4\text{V}_5\text{O}_{17}-x\text{BaV}_2\text{O}_6$  ( $x = 0.8, 0.88, 0.9$ ) composite ceramics were fabricated through a high-temperature solid phase reaction method. High-purity oxides or carbonates:  $\text{BaCO}_3$  (99%),  $\text{Na}_2\text{CO}_3$  (99.8%),  $\text{V}_2\text{O}_5$  (99%) and  $\text{CaCO}_3$  (99%) were doped as raw materials. Predried starting materials in stoichiometric  $\text{NaCa}_4\text{V}_5\text{O}_{17}$  (NCV) and  $\text{BaV}_2\text{O}_6$  (BV) compositions were mixed with ethanol in a nylon jar and stirred for 8 h using  $\text{ZrO}_2$  balls. The NCV and BV powders

were presintered under 600 °C holding for 4 h and 460 °C for 3 h, individually. Then, pre-sintered NCV and BV powders were blended in different molar fraction, and re-milled for 8 h. After drying, the mixture powders were mixed with 5 wt% polyvinylalcohol solution as binder, granulated and pressed into cylindrical disks ( $\Phi 10 \text{ mm} \times 6 \text{ mm}$ ) at 200 MPa. Finally, the  $(1-x)\text{NCV}-x\text{BV}$  disks were sintered from 525 to 600 °C with an interval of 25 °C in air.

The phase constitutions, surface morphologies and main chemical composition of fired samples along with their compatibility with Al powders were identified by powder X-ray diffraction (PXRD, Smartlab, Japan), scanning electron microscope (SEM, Gemini300, Germany) and energy dispersive spectrometer (EDS). Archimedes-method was used to gauge the bulk density of obtained ceramics. The  $\epsilon_r$ ,  $Q_{\text{xf}}$  and  $\tau_f$  values of  $(1-x)\text{NCV}-x\text{BV}$  composite were tested through a vector network analyzer (Keysight Tech., E5071C ENA) at 9.0–11.3 GHz equipped with the  $\text{TE}_{018}$  shielded cavity. The  $\tau_f$  was computed according to the following formula:

$$\tau_f = \frac{f_{85} - f_{25}}{f_{25} \times (85 - 25)} \times 10^6 \quad (1)$$

## 3. Results and discussion

**Fig. 1** gives the PXRD profiles of 800 °C sintered  $\text{NaCa}_4\text{V}_5\text{O}_{17}$  ceramics and 550 °C sintered  $(1-x)\text{NaCa}_4\text{V}_5\text{O}_{17}-x\text{BaV}_2\text{O}_6$  ( $0.8 \leq x \leq 0.9$ ) composite ceramics. As seen in **Fig. 1**, there were no extra diffraction peaks except for the diffraction peaks of  $\text{NaCa}_4\text{V}_5\text{O}_{17}$  (CCDC# 1,833,278) and  $\text{BaV}_2\text{O}_6$  (JCPDS# 86-0240), indicating that a stable  $\text{NaCa}_4\text{V}_5\text{O}_{17}-\text{BaV}_2\text{O}_6$  diphasic ceramics was achieved, as was also demonstrated by later SEM results. The good chemical compatibility between  $\text{NaCa}_4\text{V}_5\text{O}_{17}$  and  $\text{BaV}_2\text{O}_6$  could attribute to their diverse crystal structure, that is,  $\text{NaCa}_4\text{V}_5\text{O}_{17}$  exhibits a triclinic structure, whereas  $\text{BaV}_2\text{O}_6$  crystallizes in a orthorhombic structure [14,17]. The good chemical compatibility between  $\text{NaCa}_4\text{V}_5\text{O}_{17}$  and  $\text{BaV}_2\text{O}_6$  is conducive to modulation of the dielectric properties of  $\text{NaCa}_4\text{V}_5\text{O}_{17}$  matrix, particularly for its  $\tau_f$  [18], which is well presented in our cases.

**Table 1** summarizes the measured and calculated  $\epsilon_r$  and  $\tau_f$  values of 550 °C for 4 h sintered  $(1-x)\text{NaCa}_4\text{V}_5\text{O}_{17}-x\text{BaV}_2\text{O}_6$  composite ceramics. The  $\tau_f$  could be continuously tuned with the change of the blend mixture proportion of  $\text{NaCa}_4\text{V}_5\text{O}_{17}$  and  $\text{BaV}_2\text{O}_6$ . Typically, a near zero  $\tau_f$

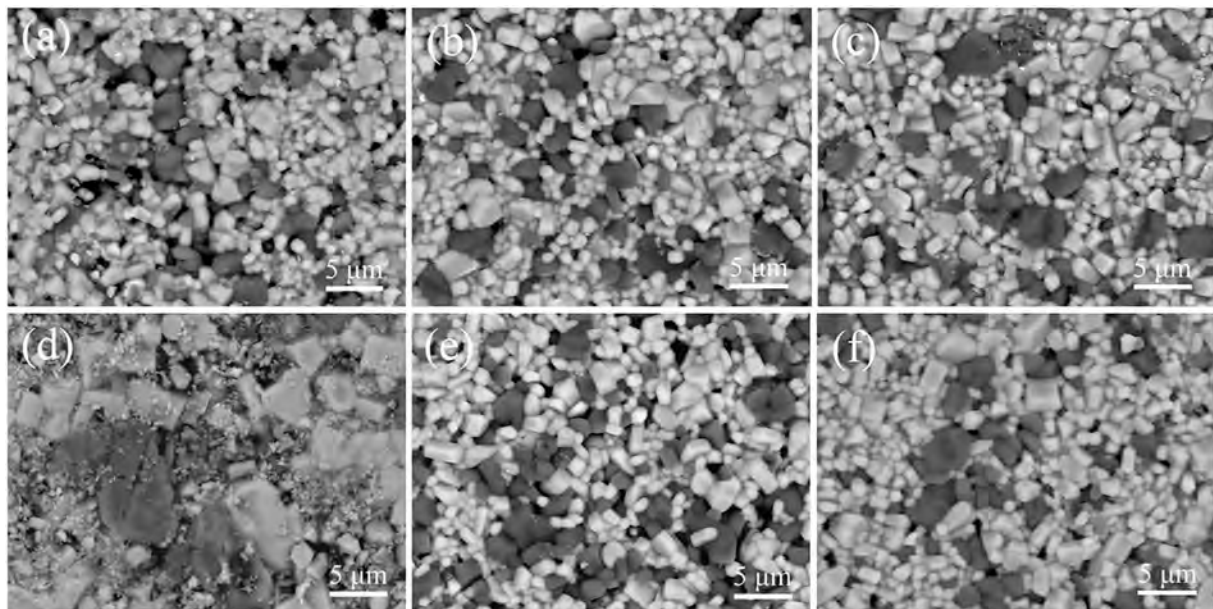


**Fig. 2.** Typical backscattered electron micrographs of  $(1-x)\text{NaCa}_4\text{V}_5\text{O}_{17}-x\text{BaV}_2\text{O}_6$  composite ceramics sintered at diverse temperatures: (a)  $x = 0.88$ , 525 °C; (b)  $x = 0.88$ , 550 °C; (c)  $x = 0.88$ , 575 °C; (d)  $x = 0.88$ , 600 °C; (e)  $x = 0.8$ , 550 °C; (f)  $x = 0.9$ , 550 °C.



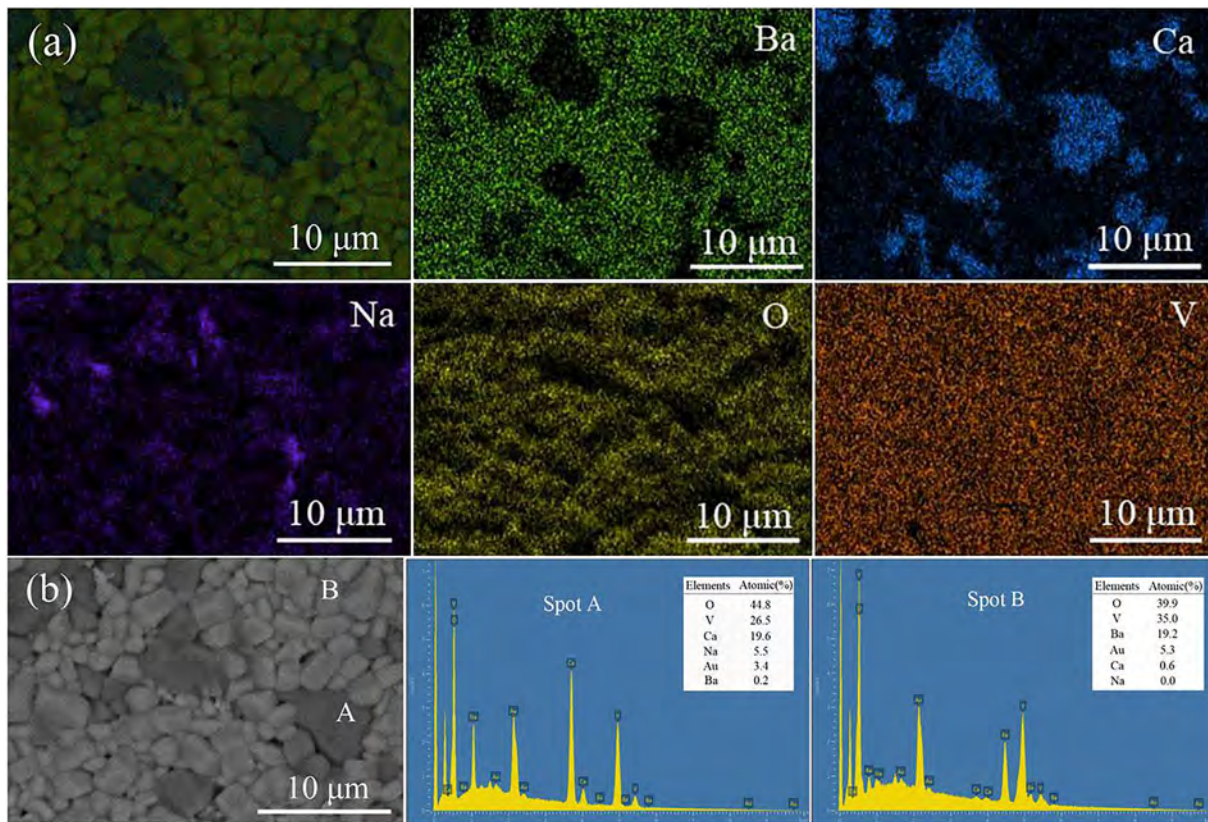


Fig. 3. (a) EDS (elements) mapping, (b) EDS spectra of  $0.12\text{NaCa}_4\text{V}_5\text{O}_{17}-0.88\text{BaV}_2\text{O}_6$  samples sintered at 550 °C.

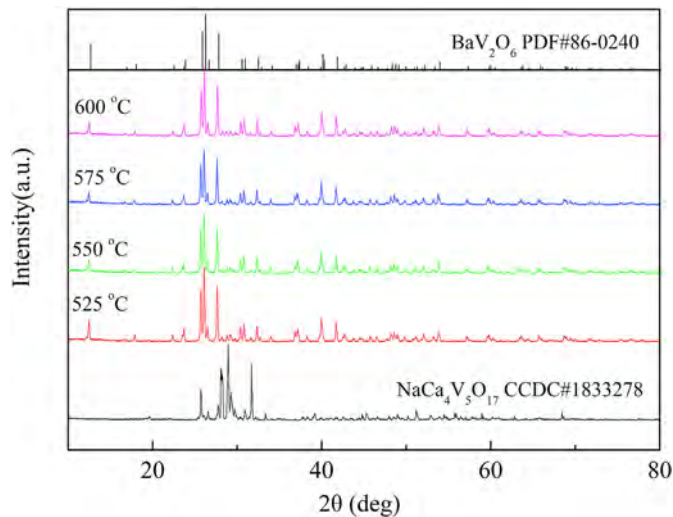


Fig. 4. PXRD patterns of  $0.12\text{NaCa}_4\text{V}_5\text{O}_{17}-0.88\text{BaV}_2\text{O}_6$  ceramics heated at different temperatures.

could be obtained for  $0.12\text{NaCa}_4\text{V}_5\text{O}_{17}-0.88\text{BaV}_2\text{O}_6$  composite ceramics.

Fig. 2 displays the typical backscattered electron micrographs of  $(1-x)\text{NaCa}_4\text{V}_5\text{O}_{17}-x\text{BaV}_2\text{O}_6$  composite ceramics sintered at diverse temperatures. A porous structure or abnormal grain growth were observed for the ceramics sintered at temperature below 550 °C or above 575 °C, respectively, which would result in low bulk density. However, from Fig. 2(b) and (c), a pretty compact microstructure without any obvious pores was obtained when samples sintered at 550–575 °C, facilitating the dielectric performance of ceramics [19]. Meanwhile, two different color grains were observed for all specimens: bright and dark grains,

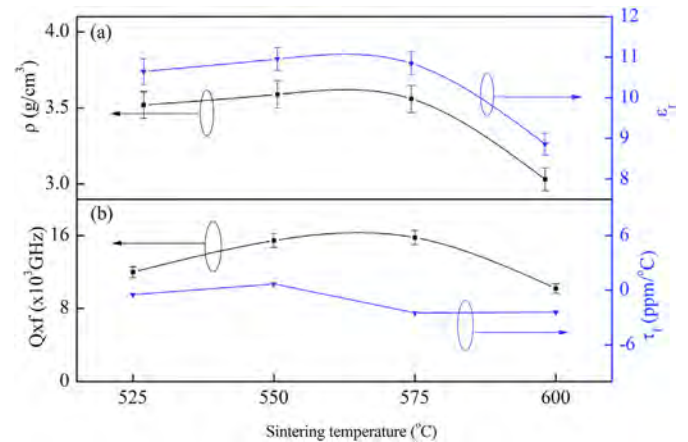


Fig. 5. Variation of the density and microwave dielectric properties of the  $0.12\text{NaCa}_4\text{V}_5\text{O}_{17}-0.88\text{BaV}_2\text{O}_6$  ceramics versus firing temperature.

indicating the different phase constitution.

EDS (elements) mapping and spectra of  $0.12\text{NaCa}_4\text{V}_5\text{O}_{17}-0.88\text{BaV}_2\text{O}_6$  samples sintered at 550 °C were conducted to identify the phase constitution of the distinct color grains. The corresponding results are presented in Fig. 3. As indicated in Fig. 3(a), the O and V elements are uniformly distributed over in all the grains, whereas the Na and Ca elements are mainly distributed on the dark grains and Ba element on the white grains, respectively. According to the quantitative EDS spectra (Fig. 3(b)), the dark (marked A) and white grains (marked B) approximately corresponded to  $\text{NaCa}_4\text{V}_5\text{O}_{17}$  and  $\text{BaV}_2\text{O}_6$  separately, which was in accordance with PXRD results.

Fig. 4 depicts the PXRD patterns of  $0.12\text{NaCa}_4\text{V}_5\text{O}_{17}-0.88\text{BaV}_2\text{O}_6$  composite ceramics heated at different temperatures. As shown in Fig. 4, with sintering temperature raised, all samples displayed mixed

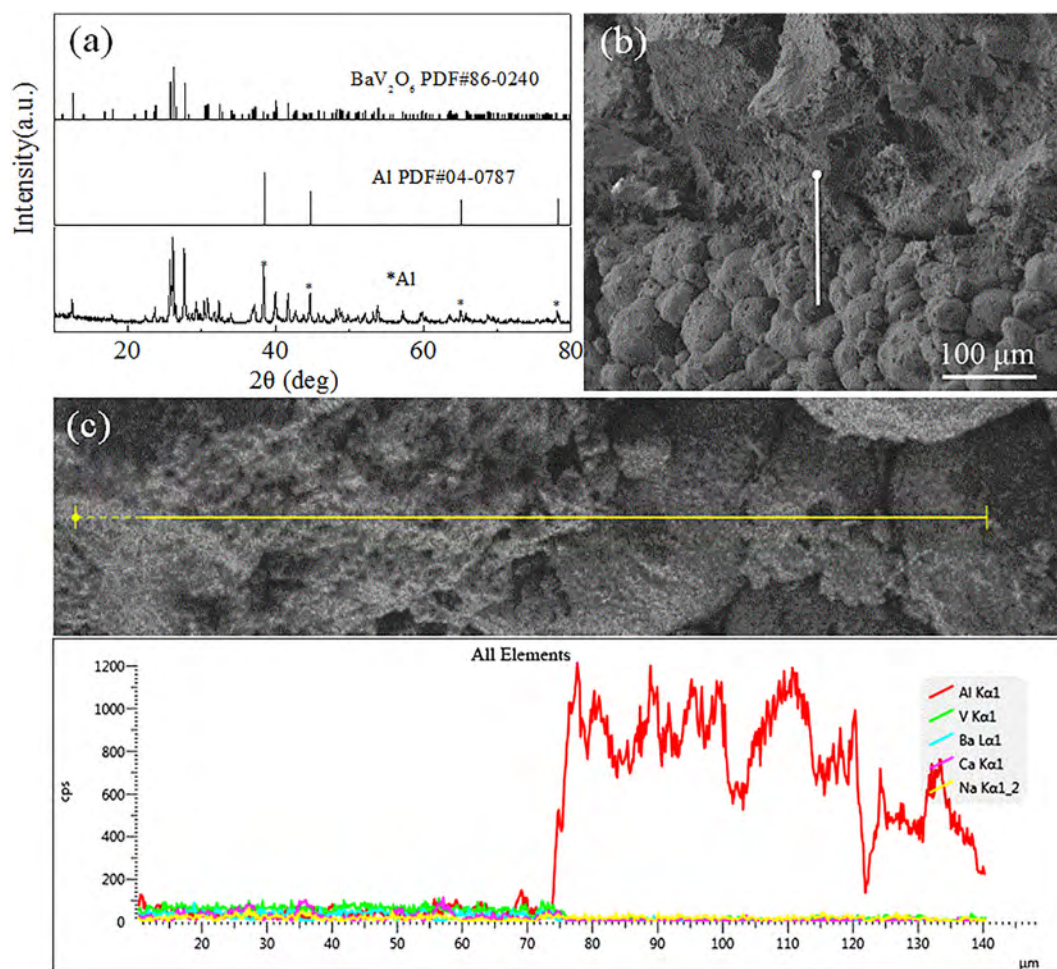


Fig. 6. (a) PXRD, (b) fracture SEM images, (c) EDS line-scans of 0.12NaCa<sub>4</sub>V<sub>5</sub>O<sub>17</sub>-0.88BaV<sub>2</sub>O<sub>6</sub> composites co-fired with 20 wt% Al powders at 550 °C.

phases and remained identical, including the main phase BaV<sub>2</sub>O<sub>6</sub> with orthorhombic structure and small amount of triclinic NaCa<sub>4</sub>V<sub>5</sub>O<sub>17</sub> phase.

The plots of dielectric properties of 0.12NaCa<sub>4</sub>V<sub>5</sub>O<sub>17</sub>-0.88BaV<sub>2</sub>O<sub>6</sub> composite ceramics versus firing temperature are represented in Fig. 5. As shown in Fig. 5 (a), the bulk density initially ascended, reached saturated values at 550–575 °C, and thereafter descended with an elevated temperature. The change in bulk density was consistent with the morphology analysis aforementioned. The changes of  $\epsilon_r$  and Qxf with an elevated temperature presented a resemble tendency as that of bulk density. The supreme values of  $\epsilon_r$  and Qxf corresponded to the maximum density, implying the close rely of  $\epsilon_r$  and Qxf on density. Thus, the elevated density may be responsible for the increment of  $\epsilon_r$  and Qxf values, whereas the rapid growth of partial grains corresponded to the decline of  $\epsilon_r$  and Qxf values [20]. In addition, as seen in Fig. 5 (b), the  $\tau_f$  value of the 0.12NaCa<sub>4</sub>V<sub>5</sub>O<sub>17</sub>-0.88 BaV<sub>2</sub>O<sub>6</sub> composite ceramics waved  $\sim -1.0$  ppm/°C indifferently to sintering temperature variation, which was due to the invariable phase composition [21]. Compared to Refs. [15], the introduction of an amount of BaV<sub>2</sub>O<sub>6</sub> in NaCa<sub>4</sub>V<sub>5</sub>O<sub>17</sub> not only improved the  $\tau_f$  value but also remarkably lowered the sintering temperature of NaCa<sub>4</sub>V<sub>5</sub>O<sub>17</sub>-basic ceramics. This may make the NaCa<sub>4</sub>V<sub>5</sub>O<sub>17</sub>-basic ceramics as a potential ULTCC material.

The chemical compatibility with Al electrode is the essential require of ULTCC material [22]. Therefore, we carried out the research on the chemical compatibility of 0.12NaCa<sub>4</sub>V<sub>5</sub>O<sub>17</sub>-0.88BaV<sub>2</sub>O<sub>6</sub> composites with Al powders. Fig. 6 shows the PXRD and fracture SEM images coupled with EDS line-scans of 550 °C sintered 0.12NaCa<sub>4</sub>V<sub>5</sub>O<sub>17</sub>-0.88BaV<sub>2</sub>O<sub>6</sub> composites doped with 20 wt% Al powders. There were no

additional phases except for those of the Al (JCPDS #04-0787) and composite ceramics, as shown in Fig. 6 (a). The interface was well maintained and no diffusion occurred between 0.12NaCa<sub>4</sub>V<sub>5</sub>O<sub>17</sub>-0.88BaV<sub>2</sub>O<sub>6</sub> and Al during the firing process, as confirmed in Fig. 6 (b) and (c). The absence deficiency of any extra phases including Al and no diffusion indicated the good chemical compatibility between 0.12NaCa<sub>4</sub>V<sub>5</sub>O<sub>17</sub>-0.88BaV<sub>2</sub>O<sub>6</sub> composites and Al electrode, suggesting it could serve in ULTCC applications.

#### 4. Conclusions

Temperature stable (1-x)NaCa<sub>4</sub>V<sub>5</sub>O<sub>17</sub>-xBaV<sub>2</sub>O<sub>6</sub> (0.8 ≤ x ≤ 0.9) have been fabricated through a conventional solid phase reaction route. The impacts of sintering temperature and composition on crystalline phases, microstructure, microwave dielectric characteristics of (1-x)NaCa<sub>4</sub>V<sub>5</sub>O<sub>17</sub>-xBaV<sub>2</sub>O<sub>6</sub> were investigated. Coexistence of NaCa<sub>4</sub>V<sub>5</sub>O<sub>17</sub> and BaV<sub>2</sub>O<sub>6</sub> phases as well as its chemical compatibility with Al powders were verified by the XRD and SEM-EDS analyses. The BaV<sub>2</sub>O<sub>6</sub> addition could improve the  $\tau_f$  and lower the sintering temperature of NaCa<sub>4</sub>V<sub>5</sub>O<sub>17</sub>-basic ceramics simultaneously. Favorable dielectric properties were achieved in the 0.12 NaCa<sub>4</sub>V<sub>5</sub>O<sub>17</sub>-0.88BaV<sub>2</sub>O<sub>6</sub> composite ceramics fired at 550 °C:  $\epsilon_r \sim 10.9$ , Qxf  $\sim 15,500$  GHz (at 10.3 GHz),  $\tau_f \sim -1.0$  ppm/°C. Its well compatible with Al electrode further rendered the 0.12NaCa<sub>4</sub>V<sub>5</sub>O<sub>17</sub>-0.88BaV<sub>2</sub>O<sub>6</sub> composites suitable for ULTCC applications.



## Declaration of competing interest

The authors declare that they have no known competing financial interests or personal relationships that could have appeared to influence the work reported in this paper.

## Acknowledgements

The authors acknowledge the financial supports of the Key Research and Development Projects of Shaanxi Provincial (2020GY-040), China Postdoctoral Science Foundation (2015M582696), Shaanxi Province Postdoctoral Science Foundation, and Xi'an Science and Technology Bureau (GXYS17.19).

## References

- [1] J.M. Li, C.G. Fan, Z.X. Cheng, S.L. Ran, Influence of Zn nonstoichiometry on the phase structure, microstructure and microwave dielectric properties of Nd ( $\text{Zn}_{0.5}\text{Ti}_{0.5}\text{O}_3$ ) ceramics, *J. Alloys Compd.* 793 (2019) 385–392.
- [2] Y.H. Zhang, J.J. Sun, N. Dai, Z.C. Wu, H.T. Wu, C.H. Yang, Crystal structure, infrared spectra and microwave dielectric properties of novel extra low-temperature fired  $\text{Eu}_2\text{Zr}_3(\text{MoO}_4)_9$  ceramics, *J. Eur. Ceram. Soc.* 39 (2019) 1127–1131.
- [3] S.B. An, J. Jiang, J.Z. Wang, L. Gan, T.J. Zhang, Microwave dielectric property modification of  $\text{Ba}_4\text{Nd}_{9.33}\text{Ti}_{18}\text{O}_{54}$  ceramics by the substitution of  $(\text{Al}_{0.5}\text{Nb}_{0.5})^{4+}$  for  $\text{Ti}^{4+}$  and the addition of  $\text{NdAlO}_3$ , *Ceram. Inter.* 46 (2020) 3960–3967.
- [4] Z.Y. Tan, H.X. Lin, K.X. Song, M.Z. Dang, X.G. Yao, H.S. Ren, T.Y. Xie, H.Y. Peng, Effects of  $\text{TiO}_2$  additive on ultra-low-loss MgO–LiF microwave dielectric ceramics, *Ceram. Inter.* 46 (2020) 5753–5756.
- [5] M. Rakhij, G. Subodh, Crystal structure, phonon modes, and bond characteristics of  $\text{AgPb}_2\text{B}_2\text{V}_3\text{O}_{12}$  (B = Mg, Zn) microwave ceramics, *J. Am. Ceram. Soc.* 103 (2020) 3157–3167.
- [6] K.G. Wang, T.T. Yin, H.F. Zhou, X.B. Liu, J.J. Deng, S.X. Li, C.M. Lu, X.L. Chen, Bismuth borate composite microwave ceramics synthesised by different ratios of  $\text{H}_3\text{BO}_3$  for LTCC technology, *J. Eur. Ceram. Soc.* 40 (2020) 381–385.
- [7] Z.B. Feng, B.J. Tao, W.F. Wang, H.Y. Liu, H.T. Wu, Z.L. Zhang, Sintering behavior and microwave dielectric properties of  $\text{Li}_4\text{Mg}_3[\text{Ti}_{0.8}(\text{Mg}_{1/3}\text{Ta}_{2/3})_{0.2}]\text{O}_9$  ceramics with LiF additive for LTCC applications, *J. Alloy, Compd* 822 (2020) 153634–153639.
- [8] M.T. Sebastian, H. Wang, H. Jantunen, Low temperature co-fired ceramics with ultra-low sintering temperature: a review, *Curr. Opin. Solid. St. M.* 20 (2016) 151–170.
- [9] H.H. Guo, D. Zhou, L.X. Pang, Z.M. Qi, Microwave dielectric properties of low firing temperature stable scheelite structured  $(\text{Ca,Bi})(\text{Mo,V})\text{O}_4$  solid solution ceramics for LTCC applications, *J. Eur. Ceram. Soc.* 39 (2019) 2365–2373.
- [10] R. Naveenraj, E.K. Suresh, J. Dhanya, R. Ratheesh, Preparation and microwave dielectric properties of  $\text{Ba}_3\text{A}(\text{V}_2\text{O}_7)_2$  (A = Mg, Zn) ceramics for LTCC applications, *Eur. J. Inorg. Chem.* (2019) 949–955 2019.
- [11] A. Sasidharanpillai, S.M. Thomas, Y. Lee, H.T. Kim, Ultra-low temperature co-fired  $\text{CaV}_2\text{O}_6$ -glass composite ceramic substrate for microelectronics, *J. Mater. Sci. Mater. Electron.* 30 (2019) 7634–7644.
- [12] K. Cheng, C.C. Li, C.Z. Yin, Y. Tang, Y.H. Sun, L. Fang, Effects of  $\text{Sr}^{2+}$  substitution on the crystal structure, Raman spectra, bond valence and microwave dielectric properties of  $\text{Ba}_{3-x}\text{Sr}_x(\text{VO}_4)_2$  solid solutions, *J. Eur. Ceram. Soc.* 39 (2019) 3738–3743.
- [13] P. Atousa, T.N. Ehsan, T.A. Hamid, W.Z. Lu, W. Lei, H.B. Bafrooei, Study on structure, microstructure, and microwave dielectric characteristics of  $\text{CaV}_2\text{O}_6$  and  $(\text{Ca}_{0.95}\text{M}_{0.05})\text{V}_2\text{O}_6$  (M = Zn, Ba) ceramics, *J. Am. Ceram. Soc.* 102 (2019) 5213–5222.
- [14] Z.Q. Xie, S.C. Cheng, S.W. Li, H.Q. Ding,  $\text{NaCa}_4\text{V}_5\text{O}_{17}$  with isolated  $\text{V}_2\text{O}_7$  dimer and  $\text{V}_3\text{O}_{10}$  trimer exhibiting a large birefringence, *J. Solid State Chem.* 269 (2019) 94–99.
- [15] C.Z. Yin, C.C. Li, L. Fang, et al.,  $\text{NaCa}_4\text{V}_5\text{O}_{17}$ : a low-firing microwave dielectric ceramic with low permittivity and chemical compatibility with silver for LTCC applications, *J. Eur. Ceram. Soc.* 40 (2020) 386–390.
- [16] G.G. Yao, Y. Li, J.J. Tan, C.J. Pei, Y. Zhang, J. Chen, Effects of  $\text{V}_2\text{O}_5$  on sinterability and microwave dielectric properties of  $\text{NaCa}_4\text{V}_5\text{O}_{17}$  ceramics, *J. Ceram. Process. Res.* 21 (2020) 1–5.
- [17] U.A. Neelakantan, S.E. Kalathil, R. Ratheesh, Structure and microwave dielectric properties of ultralow-temperature cofirable  $\text{BaV}_2\text{O}_6$  ceramics, *Eur. J. Inorg. Chem.* 2015 (2015) 305–310.
- [18] G.G. Yao, C.J. Pei, H. Ma, J.G. Xu, P. Liu, H.W. Zhang, Low-temperature firing and microwave dielectric properties of  $(1-x)\text{Ca}_5\text{Mg}_4(\text{VO}_4)_6-x\text{Ba}_3(\text{VO}_4)_2$  temperature stable ceramics, *J. Alloys Compd.* 709 (2017) 234–239.
- [19] S.P. Wu, D.F. Chen, C. Jiang, Y.X. Mei, Q. Ma, Synthesis of monoclinic  $\text{CaSnSiO}_5$  ceramics and their microwave dielectric properties, *Mater. Lett.* 91 (2013) 239–241.
- [20] Z.W. Zhang, Y. Tang, J. Li, J.Q. Chen, A.H. Yang, Y. Wang, Y.F. Zhai, L.Y. Ao, C.X. Su, X.R. Xing, L. Fang, High-Q and near-zero  $\tau_f$  composite  $\text{Li}_2\text{Mg}_2\text{TiO}_5$ - $\text{Sr}_3(\text{VO}_4)_2$  ceramics for low temperature co-fired ceramic applications, *Ceram. Inter.* 46 (2020) 8281–8286.
- [21] J.Q. Ren, K. Bi, X.L. Fu, Z.J. Peng, Novel  $\text{Al}_2\text{Mo}_3\text{O}_{12}$ -based temperature-stable microwave dielectric ceramics for LTCC applications, *J. Mater. Chem. C.* 6 (2018) 11465–11470.
- [22] M. Valant, O. Popovic, M.V. Mihelj, S. Burazer, A. Altomare, A. Moliterni, Oxide crystal structure with square-pyramidally coordinated vanadium for integrated electronics manufactured at ultralow processing temperatures, *ACS Sustain. Chem. Eng.* 5 (2017) 5662–5668.